Łukasz TOPOLSKI, Jurij WARECKI, Zbigniew HANZELKA

AGH University of Science and Technology

doi:10.15199/48.2018.09.21

Methods for determining power losses in cable lines with non-linear load

Abstract. *Harmonic currents in power cables cause additional power losses associated with phenomena that increase the temperature of the cable insulation and make its service life shorter. For these reasons, it is important to choose methods for determining active power losses, which ensure adequate computational accuracy. This paper compares the methods for determining active power losses on the example of a low voltage cable line supplying a non-linear load.*

Streszczenie. *Przepływ wyższych harmonicznych prądu przez linie kablowe skutkuje powstawaniem dodatkowych strat mocy czynnej związanych z ujawnianiem się niekorzystnych zjawisk, które prowadzą do wzrostu temperatury izolacji oraz skrócenia czasu jej życia. Z powyższych względów ważną kwestią staje się wybór metod wyznaczania strat mocy czynnej zapewniających odpowiednią dokładność obliczeń. W artykule przeprowadzono porównanie metod wyznaczania strat mocy czynnej na przykładzie linii kablowej niskiego napięcia zasilającej nieliniowe obciążenie. (**Metody wyznaczania strat w liniach kablowych z obciążeniem nieliniowym**).*

Keywords: higher harmonics, skin effect, proximity effect, additional power losses.
Słowa kluczowe: wyższe harmoniczne, zjawisko naskórkowości, efekt zbliżenia, dodatkowe straty mocy.

Introduction

Polyethylene (PE) has been used as electrical insulation in underground distribution and transmission class power cables for over three decades. The polyethylene in power cables is a special grade, which has cross-linked molecules to allow it to deal with extremely high temperatures without melting or flowing under load. The operating temperature of XLPE insulated power cables is 90 ^{o}C and its service life is estimated at approximately 30 years under purely sinusoidal currents. The flow of harmonic currents through power cable causes additional active power losses associated with the higher rms value of current and the appearance of adverse phenomena, which include the skin effect, the proximity effect and the impact of the metallic cable screen (shield), which, in turn, lead to increased insulation temperature and shorter cable service life.

Failures of commonly used power cable are a great nuisance for consumers and a cause of considerable financial losses for companies. Due to the above, it is becoming increasingly more important to define accurate, fast and simple methods for determining additional power losses, in order to reduce power cable line load with the fundamental current harmonic, to prevent it from overheating.

The aim of this paper is to analyse methods for determining active power losses in cable lines with single-strand and multi-strand conductors, operating in environment rich in current harmonics. By way of example, authors performed calculations of the active power losses for an actual low voltage power cable line supplying an electrostatic precipitator assembly in an industrial facility. The results obtained with different methods were compared and discussed.

Nature of cable losses under a non-linear load

Power losses in cable lines are Joule's losses, caused by the current flowing through a conductor. The basic term describing Joule's losses is defined as a product of the value of current square and conductor resistance ($I^2 * R$). In case of supplying a non-linear load, the current of that load contains higher harmonics, and the resistance become dependent on the frequency. That dependency of resistance on current frequency is one of the causes for the additional power losses in power cable lines.

The value of equivalent resistance of a conductor for alternating current is impacted by the following physical phenomena. The first phenomenon is the skin effects, which reveal that the current in a conductor does not flow evenly throughout the entire cross-section but only a part of it, depending on the current frequency (fig. 1). The higher the frequency, the closer the current flows to the outer surface of the conductor (current density decreases from the surface towards the inside).

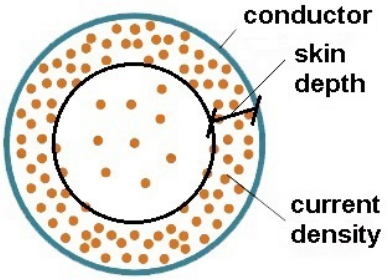

Fig. 1. Skin effect visualization

The skin effect is mainly caused by eddy currents originating from the electromotive force induced in a conductor by the electromagnetic field generated by the primary current flowing through the conductor. Eddy currents cause the primary current to fade in the center of the conductor and strengthen the flow in its upper layers.

Another physical phenomenon impacting the resistance of a conductor is the proximity effect. The effect appears in sets of two or more conductors located close to each other. If the current in the conductors flows in the same direction, the biggest current density appears in the conductor parts most remote from each other (fig. 2). In contrast, when the current flows in opposite directions, the biggest current density can be found in conductor parts closest to each other (fig. 3).

The proximity effect, similar to the skin effect, is also caused by eddy currents. Primary current flowing through one of the conductors generates a time varying magnetic field, which then induces electromotive force in the second conductor, which, in turn, forces the flow of eddy currents, causing primary current densification in a part of the conductor depending on its flow direction.

Both the skin effect and the proximity effect cause the current density to be nonuniform in the cross-section of the conductor and cause higher cable losses.

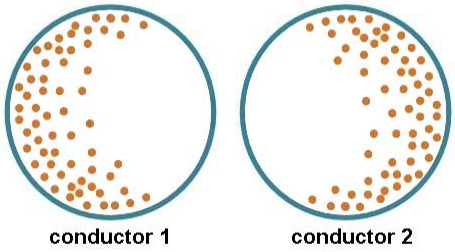

Fig. 2. Proximity effect visualization for coherent current flow directions

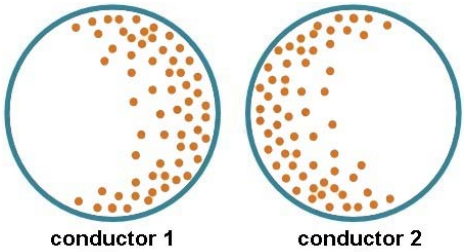

Fig. 3. Proximity effect visualization for opposite current flow directions

The increase in active power losses in a cable line is also influenced by a phenomenon caused by the impact of the metallic cable screen (shield) (if a given cable has it). Primary current flowing through an operating conductor induces electromagnetic force in a metallic cable screen (shield), forcing the flow of eddy currents in this part of the cable, which results in additional active power losses and increased temperature, thus limiting the maximum capacity of the cable line.

Resistance determination methods

Cable conductor resistance for harmonic current h, with respect to the skin effect, the proximity effect and the impact of the metallic cable screen (shield), is expressed by the relationship [1,3,5,7]

$$R_{AC}(h) = R_{DC}\left[1 + x_s(h) + x_p(h) + x_a(h)\right] \tag{1}$$

where: R_{DC} – DC conductor resistance [Ω], x_s – resistance increment in a cable conductor caused by the skin effect, x_p – resistance increment in a cable conductor caused by the proximity effect, x_a – resistance increment in a cable conductor caused by the impact of the metallic cable screen (shield).

In order to determine the resistance increment coefficients due to the skin effect, the following methods are applied for practical computations.

S1 Method. The cable conductor resistance increment coefficient, with respect to the skin effect, is determined with the use of the Bessel functions [1, 3, 5, 7]

$$x_{s1}(h) = \mathrm{Re}\left[\frac{z_s}{2}\cdot\frac{J_0(z_s)}{J_1(z_s)}\right] - 1 \tag{2}$$

$$z_s = exp\left(j\frac{3\pi}{4}\right)\cdot\sqrt{2\mu\gamma k_s sfh} \tag{3}$$

where: μ – magnetic permeability of a cable conductor material [H/m], γ – conductor conductivity [m/Ω*m^2], k_S – correction coefficient depending on a cable conductor design (k_S = 1 – single-strand conductor and k_S = 0,4 – multi-strand conductor), s – cable conductor cross-section [m^2], f – grid rated frequency [Hz], h – harmonics order, J_0, J_1 – Bessel functions of the first kind of zero and one order, respectively.

S2 Method. According to this method, the cable conductor resistance increment coefficient, with respect to the skin effect is determined by the dependence [8]

$$x_{s2}(h) = \left(\frac{l\rho}{\pi(d-\delta)\delta R_{DC}}\right) - 1 \tag{4}$$

$$\delta = \sqrt{\frac{2\rho}{2\pi f\mu h}} \tag{5}$$

where: l – cable length [m], ρ – conductor resistivity [Ω*m], d – conductor diameter [m], δ – skin depth [m].

The relationship (4) holds true, if the condition $d \gg \delta$ is met.

S3 Method. The cable conductor resistance increment coefficient caused by the skin effect is determined based on the relationship [4]

$$x_{s3}(h) = \left(\sqrt[6]{\left(\frac{3}{4}\right)^6 + \left(\frac{s}{p\delta}\right)^6} + 0,25\right) - 1 \tag{6}$$

where: p – conductor circumference [m].

S4 Method. The international standard IEC-60287-1-1 [6] recommends determining the resistance increment coefficient with respect to the skin effect, based on the relationship

$$x_{s4}(h) = \frac{y_s^4}{192 + 0,8y_s^4} \tag{7}$$

$$y_s^4 = \left(\frac{8\pi hfk_s}{R_{DC}10^7}\right)^2 \tag{8}$$

The cable conductor resistance increment coefficients, due to the proximity effect, may be determined with the use of the following methods.

P1 Method. Calculating the resistance increment coefficient based on the Bessel functions [1, 3, 5, 7]

$$x_{p1}(h) = F(z_P)\left(\frac{d}{D}\right)^2\left[\frac{1,18}{F(z_P)+0,27} + 0,312\left(\frac{d}{D}\right)^2\right] \tag{9}$$

where

$$F(z_P) = \mathrm{Re}\left[\frac{z_P J_0(z_P)}{2J_1(z_P)}\right] - 1 \tag{10}$$

$$z_P = exp\left(j\frac{3\pi}{4}\right)\cdot\sqrt{2\mu\gamma k_P sfh} \tag{11}$$

where: k_P – correction coefficient depending on the cable conductor design (kp = 1 – single-strand conductor kp = 0,3 – multi-strand conductor), D – distance between axes of conductors [m].

P2 Method. The international standard IEC-60287-1-1 [6] recommends determining the cable conductor resistance increment coefficient, with respect to the proximity effect, based on the relationship

(12) $$x_{p2}(h)=\frac{y_P^4}{192+0,8y_P^4}\left(\frac{d}{D}\right)^2\left[0,312\left(\frac{d}{D}\right)^2+\frac{1,18}{\frac{y_P^4}{192+0,8y_P^4}+0,27}\right]$$

(13) $$y_p^4=\left(\frac{8\pi hfk_P}{R_{DC}10^7}\right)^2$$

The cable conductor resistance increment coefficient, due to the impact of a metallic cable screen (shield), is determined by the dependence [1]

(14) $$x_a(h)=0,5\cdot\left[x_s(h)+x_p(h)\right]$$

Determination of power losses in cable lines

Active power losses under the flow of distorted current by a three-phase four-conductor cable line with the same cross-section area are a sum of losses in the phase conductors ΔP_L and the neutral conductor ΔP_N [4]

(15) $$\Delta P=\Delta P_L+\Delta P_N$$

Power losses in the phase conductors and the neutral conductor can be divided into loss components for the fundamental (h = 1) and higher harmonics current (h = 2,3,…) in the form of

(16) $$\Delta P_L=\Delta P_{L1}+\Delta P_{Lh}$$

(17) $$\Delta P_N=\Delta P_{N1}+\Delta P_{Nh}$$

where

(18) $$\Delta P_{L1}=R_{DC}\left(I_{A1}^2+I_{B1}^2+I_{C1}^2\right)$$

(19) $$\Delta P_{Lh}=\sum_{h=2}^{h=\infty}R_{AC}(h)\cdot\left(I_{Ah}^2+I_{Bh}^2+I_{Ch}^2\right)$$

and

(20) $$\Delta P_{N1}=R_{DC}\cdot I_{N1}^2$$

(21) $$\Delta P_{Nh}=\sum_{h=2}^{h=\infty}R_{AC}(h)\cdot I_{Nh}^2$$

where: I_{A1}, I_{B1}, I_{C1} – rms values of fundamental harmonic phase currents [A], I_{N1} – rms value of fundamental harmonic neutral conductor current [A], ΔP_{Lh}, ΔP_{Nh} – additional power losses in the phase conductors and the neutral conductor [W].

When distorted currents flow through a cable line, the rms values of currents are determined with the relationships

(22) $$I_F=\sqrt{\sum_{h=1}^{h=\infty}I_{Fh}^2}$$

(23) $$I_N=\sqrt{\sum_{h=1}^{h=\infty}I_{Nh}^2}$$

where: I_F – rms value of distorted phase current ($F \in A, B, C$) [A], I_N – rms value of distorted neutral conductor current [A].

Active power loss increase caused by the flow of distorted current in proportion to the losses caused by the flow of the fundamental harmonic current is determined by the relationship [1]

(24) $$\Delta P_{h\%}=\frac{\Delta P-\left(\Delta P_{L1}+\Delta P_{N1}\right)}{\Delta P_{L1}+\Delta P_{N1}}\cdot 100\%$$

According to [2] a derating factor for a cable line with flowing symmetrical distorted currents is calculated based on the assumption that I_{F1} is an rms value of fundamental harmonic current

(25) $$3I_F^2\cdot R_{DC}=3I_{F1}^2\cdot R_{DC}+\Delta P_{Lh}+\Delta P_{Nh}$$

hence

(26) $$d_r=\frac{I_{F1}}{I_F}=\frac{1}{\sqrt{1+\frac{\Delta P_{Lh}+\Delta P_{Nh}}{\Delta P_1}}}=\frac{1}{\sqrt{1+\frac{\Delta P_{h\%}}{100}}}$$

Comparison of loss determination methods on a selected example

Description of the analysed object

The selected example is a four-conductor low voltage cable line supplying an electrostatic precipitator assembly operating in a cogeneration industrial plant. Apart from the electrostatic precipitator assembly, the cable line also supplies such load as rappers, electrostatic precipitator substation lighting, welding sockets, monitoring, control cabinets and external lighting [9].

The calculations involved a comparison of the supply systems with a YAKXS 4x185mm^2 cable line (without a metallic screen), with single-strand sectoral SE and multi-strand RMC aluminum conductors. The length of the cable line in the analysed system is 300 metres. Table 1 shows the specifications of the cable line supplying the electronic precipitator assembly.

Table 1. Specifications of a YAKXS 4x185mm^2 cable

Cable cross-section [mm^2]	Rated thickness [mm^2]		Outer diameter [mm]	Conductor resistance R_{DC} [Ω/km]
	insula--tion	layer		
4x185mm^2	2	2,7	46,4	0,164
Cable lenght [m]	300			

Figure 4 shows a cross-section of the analysed cable line.

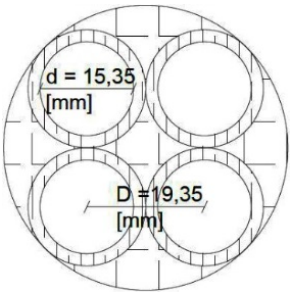

Fig. 4. Cross-section of a YAKXS 4x185 mm^2 cable developed based on the specifications [10]

Figure 5 shows a schematic diagram of the electrostatic precipitator assembly supply system.

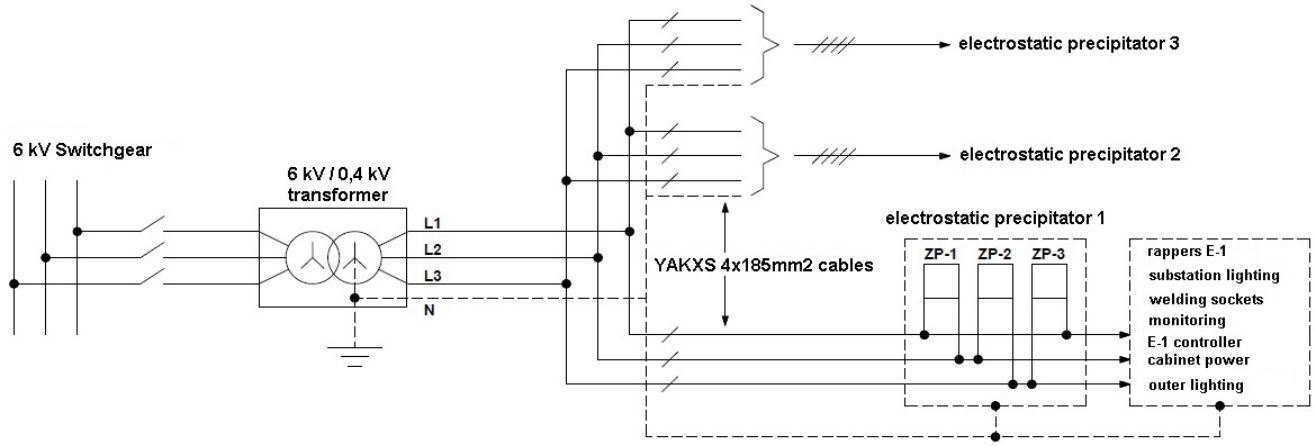

Fig. 5. Electrostatic precipitator power supply system diagram [9]

In table 2 are given rms values of higher harmonics current and the THD_I coefficient of current recorded at peak load in low voltage switchgear, supplying the electrostatic precipitator assembly.

Table 2. RMS values of higher harmonic currents recorded in an electrostatic precipitator assembly power supply system [9]

Harmonic order h	RMS value of harmonic current I_h [A]	THD_I [%]
1	327,65	29,94
2	8,06	
3	81,32	
4	5,34	
5	50,85	
6	2,79	
7	11,53	
9	6,78	
11	7,96	
13	6,03	
15	5,24	
17	1,83	
19	2,10	
21	1,80	
23	1,25	
25	1,57	

Comparison of resistance increments determination methods

Using the methods S1-S4, the resistance increments of a single-strand sectoral SE cable conductor were determined. The results obtained are shown in figure 7.

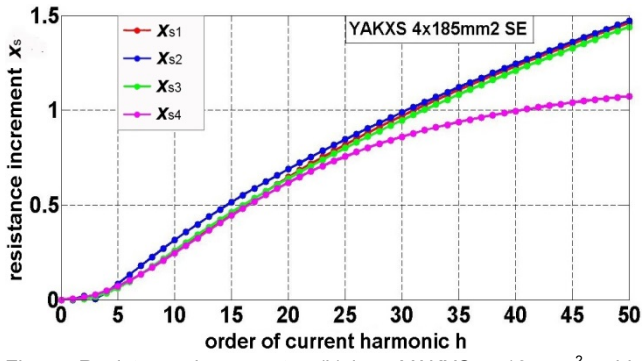

Fig. 7. Resistance increment $x_s(h)$ in a YAKXS 4x185mm^2 cable single-strand sectoral SE conductor

Based on figure 7, it can be seen that resistance increments determined with methods S1-S3 provide very similar results for the entire spectrum of higher harmonics present in the system. The biggest discrepancies were obtained when using the S4 method, which become even bigger with increasing harmonic order.

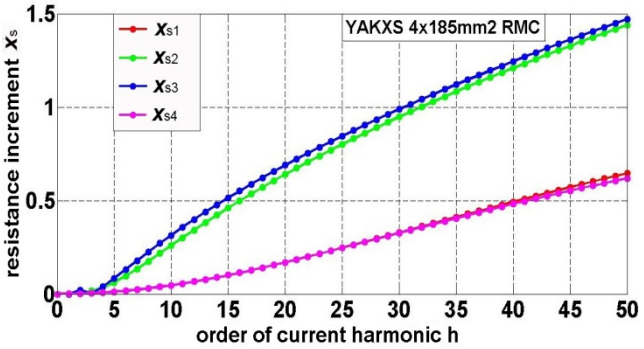

Fig. 8. Resistance increment $x_s(h)$ in a YAKXS 4x185mm^2 cable mutli-strand RMC conductor

Figure 8 also shows resistance increments due to skin effect, but for multi-strand RMC conductor. It can be noted that results of resistance increment most convergent with the S1 method were obtained using the S4 method. This is due to the fact that methods S1 and S4 include correction coefficients, which depend on the design of a cable conductor. Whereas methods S2 and S3 do not have such coefficients.

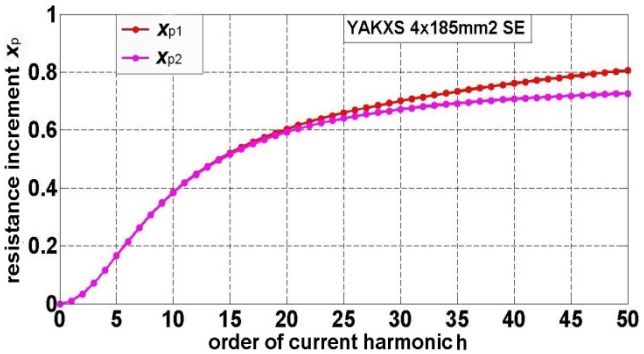

Fig. 9. Resistance increment $x_p(h)$ in a YAKXS 4x185mm^2 cable single-strand sectoral SE conductor

Figure 9 shows resistance increments for a single-strand sectoral SE conductor due to the proximity effect. As can be noted, resistance increment determined with the P2 method using the relationships recommended by the international standard IEC-60287-1-1 is very similar to the resistance increment determined with the P1 method. A minor increase of the discrepancies between the two methods can be seen from about the 20th harmonic.

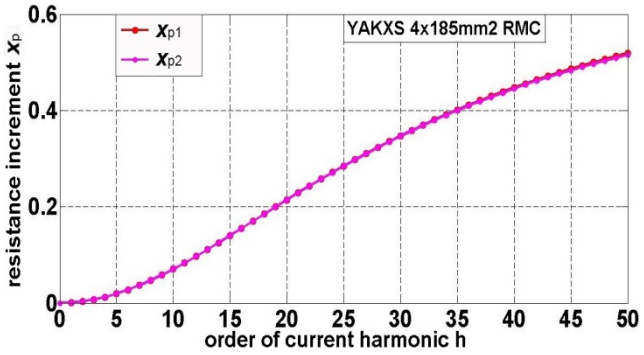

Fig. 10. Resistance increment $x_p(h)$ in a YAKXS 4x185mm^2 cable mutli-strand RMC conductor

Figure 10 also presents resistance increments due to the proximity effect, but in a multi-strand RMC conductor. In this case, regardless of the method selected, the results obtained are identical for the entire harmonics spectrum.

Resistance increments for a single-strand sectoral SE cable conductor, with respect to the skin effect and the proximity effect are shown in figure 11.

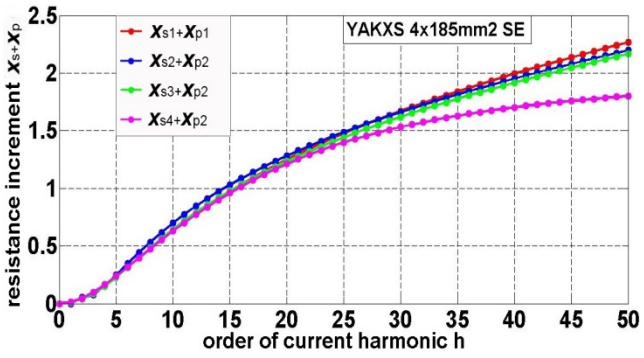

Fig. 11. Total resistance increment $x_s(h)+x_p(h)$ in a YAKXS 4x185mm^2 cable single-strand sectoral SE conductor due to the impact of higher harmonics

As can be seen in figure 11, the most divergent resistance increments values were obtained when using the relationships recommended by the international standard IEC-60287-1-1 (a combination of methods S4 and P2).

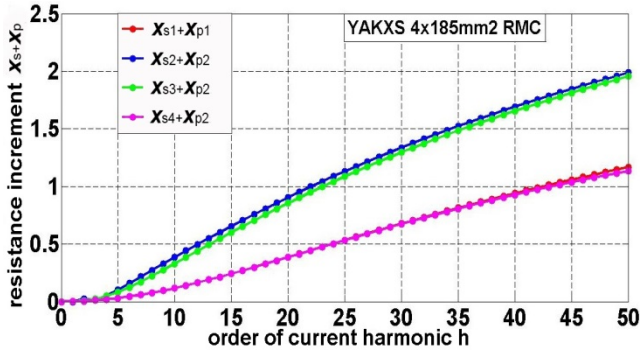

Fig. 12. Total resistance increment $x_s(h)+x_p(h)$ in a YAKXS 4x185mm^2 cable multi-strand RMC conductor due to the impact of higher harmonics

In contrast, for a multi-strand conductor cable (fig. 12), the situation is different. In this case, resistance increments values most convergent with the increments obtained with the Bessel functions (a combination of methods S1 and P1) were obtained using the relationships recommended by the international standard IEC-60287-1-1 (a combination of methods S4 and P2).

Power losses in a cable line

Using the determined total resistance increments for a cable conductor (fig. 11 and fig. 12), and based on the relationships (15) – (26), the power losses for the cable line in question, a percentage loss increments and a derating factors were determined. The loss computations were conducted for two cases – assuming the absence of higher harmonics in the system and assuming their presence.

The computations assumed that the electrostatic precipitator assembly is a symmetrical load; hence, the fundamental current harmonic does not flow through the neutral conductor. Calculation results are shown in tables 3 and 4.

Table 3. Power losses, percentage loss increments and derating factors in a YAKXS 4x185mm^2 cable line with single-strand sectoral SE conductors

Calculation method	S1+P1	S2+P2	S3+P2	S4+P2
ΔP_{L1} [kW]	15,85	15,85	15,85	15,85
ΔP_{Lh} [kW]	1,64	1,62	1,62	1,64
ΔP_{N1} [kW]	0,00	0,00	0,00	0,00
ΔP_{Nh} [kW]	3,28	3,21	3,25	3,28
ΔP [kW]	20,77	20,68	20,72	20,77
$\Delta P_{h\%}$ [%]	31,04	30,47	30,73	31,04
dr	0,87	0,88	0,87	0,87

Table 4. Power losses, percentage loss increments and derating factors in a YAKXS 4x185mm^2 cable line with multi-strand RMC conductors

Calculation method	S1+P1	S2+P2	S3+P2	S4+P2
ΔP_{L1} [kW]	15,85	15,85	15,85	15,85
ΔP_{Lh} [kW]	1,45	1,49	1,49	1,45
ΔP_{N1} [kW]	0,00	0,00	0,00	0,00
ΔP_{Nh} [kW]	3,00	3,02	3,05	3,00
ΔP [kW]	20,30	20,36	20,39	20,30
$\Delta P_{h\%}$ [%]	28,08	28,45	28,64	28,08
dr	0,88	0,88	0,88	0,88

Conclusions

The paper discusses the causes of additional active power losses in cable lines supplying non-linear loads, and presents and compares the methods used to determine them. Based on the analysis conducted, the following conclusions can be formulated:

1) The design of cable conductors impacts loss size. Multi-strand conductors are characterized by lower resistance increments, which results in smaller losses compared to single-strand sectoral conductors.
2) Power losses, both for a single-strand and a multi-strand cable conductors, are characterized by small discrepancies, regardless of the selected resistance increment determination method. This is associated with the fact that the electrostatic precipitator power supply system contained current harmonics of up to the 25th order, and harmonics of up to the 15th order had significant amplitudes. All of the presented methods for the determination of increment coefficients for resistances up to the 15th harmonic are characterized by small discrepancies between the values obtained; hence, the differences in the resulting losses are minor.
3) When determining losses in cable lines with single-strand conductors, operating in an environment with current harmonics with the majority of amplitudes up to circa 20th order, any resistance increment coefficient determination method can be applied. Whereas, in the presence of current harmonics above the 20th order, methods S1 – S3 and P1 – P2 are recommended to be used for the determination of resistance increments. The relationships defined in method S4 in this range of

harmonics lower the resistance increment, which will lead to lower power loss results.

4) When determining the losses in cable lines with multi-strand conductors, the relationships recommended by the international standards IEC-60287-1-1 can be used as a method for the determination of resistance increment coefficients alternative to the methods based on Bessel functions (combination of the S1 and P1 methods).

***Authors**: mgr inż. Łukasz Topolski, Akademia Górniczo-Hutnicza w Krakowie, Wydział Elektrotechniki, Automatyki, Informatyki i Inżynierii Biomedycznej, Katedra Energoelektroniki i Automatyki Systemów Przetwarzania Energii, Al. Mickiewicza 30, 30-059 Kraków, E-mail:* lukas.topolski@gmail.com*; prof. dr hab. inż. Jurij Warecki, Akademia Górniczo-Hutnicza w Krakowie, Wydział Energetyki i Paliw, Katedra Podstawowych Problemów Energetyki, Al. Mickiewicza 30, 30-059 Kraków, E-mail:* jwarecki@agh.edu.pl*; prof. dr hab. inż. Zbigniew Hanzelka, Akademia Górniczo-Hutnicza w Krakowie, Wydział Elektrotechniki, Automatyki, Informatyki i Inżynierii Biomedycznej, Katedra Energoelektroniki i Automatyki Systemów Przetwarzania Energii, Al. Mickiewicza 30, 30-059 Kraków, E-mail:* hanzel@agh.edu.pl

REFERENCES

[1] Degeneff R.C., Halleran T.M., McKernan T.M., Palmer J.A., Pipe – type cable ampacities in the presence of Harmonics. *IEEE Transactions on Power Delivery*, 8 (1993), No. 4, 1689 – 1695

[2] Demoulias C., Labridis D. P., Dokopoulos P. S., Gouramanis K. Ampacity of Low-Voltage Power Cables Under Nonsinusoidal Currents, *Power Delivery IEEE Transactions* on, 22 (2007), 584-594

[3] Desmet J. et al., Simulations of losses in LV cables due to nonlinear loads, Power Electronics Specialists Conference, PESC 2008, IEEE Conference, 2008, 785 – 790

[4] Ducluzaux A., Cahier technique no.83 – Extra losses caused in high current conductors by skin and proximity effects, Schneider Electric, (2002), 7

[5] Hiranandani A., Calculation of cable ampacities including the effects of harmonics, *IEE Industry Applications Magazine,* 4 (1998), No. 2, 42-51

[6] IEC 60287-1-1, Electric cables – Calculation of current rating – Part 1: Current rating equations (100% load factor) and calculation of losses – Section 1: General, 2006.

[7] Kot A., Nowak W., Szpyra W., Tarko R., Analysis of impact of nonlinear loads on losses in power network element, *Przegląd Elektrotechniczny*, 88 (2012), nr 8, 327 – 328

[8] Popovic Z., Popovic D., Chapter 20 The Skin Effect, *Introductory Elektromagnetics,* Prentice – Hall, ISBN 978 – 0201326789, 1999, 387

[9] Warecki J., Hanzelka Z., Gajdzica M., Wskaźniki jakości dostawy energii elektrycznej w sieci zasilającej elektrofiltry przemysłowe – analiza przypadku, *Przegląd Elektrotechniczny*, 90 (2014), nr 4, 86 – 87

[10] Tele-Fonika Kable S.A., Kable i przewody elektroenergetyczne, Katalog 2015, 157